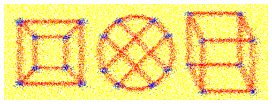
Journal of Graph Algorithms and Applications
http://jgaa.info/ vol. 24, no. 2, pp. 105–131 (2020)
DOI: 10.7155/jgaa.00521

Drawing Clustered Planar Graphs on Disk Arrangements

Tamara Mchedlidze[1] *Marcel Radermacher*[1]
Ignaz Rutter[2] *Nina Zimbel*

[1]Department of Computer Science,
Karlsruhe Institute of Technology, Germany
[2]Department of Computer Science and Mathematics,
University of Passau, Germany

Abstract

Let $G = (V, E)$ be a planar graph and let $\mathcal{V}$ be a partition of V. We refer to the graphs induced by the vertex sets in $\mathcal{V}$ as *clusters*. Let $\mathcal{D}_\mathcal{C}$ be an arrangement of pairwise disjoint disks with a bijection between the disks and the clusters. Akitaya et al. [2] give an algorithm to test whether $(G, \mathcal{V})$ can be embedded onto $\mathcal{D}_\mathcal{C}$ with the additional constraint that edges are routed through a set of pipes between the disks. If such an embedding exists, we prove that every clustered graph and every disk arrangement without pipe-disk intersections has a planar straight-line drawing where every vertex is embedded in the disk corresponding to its cluster. This result can be seen as an extension of the result by Alam et al. [3] who solely consider biconnected clusters. Moreover, we prove that it is $\mathcal{NP}$-hard to decide whether a clustered graph has such a straight-line drawing, if we permit pipe-disk intersections, even if all disks have unit size. This answers an open question of Angelini et al. [4].

Submitted:	Reviewed:	Revised:	Accepted:
April 2019	June 2019	July 2019	September 2019
	Final:	Published:	
	February 2020	February 2020	
Article type:		Communicated by:	
Regular paper		K. Mukhopadhyaya and S.-i. Nakano	

Work was partially supported by grant WA 654/21-1 of the German Research Foundation (DFG). A preliminary version of this paper appeared in the *Proceedings of the 13th International Conference and Workshops on Algortihms and Computation (WALCOM '19) [12].*
E-mail addresses: mched@iti.uka.de (Tamara Mchedlidze) radermacher@kit.edu (Marcel Radermacher) rutter@fim.uni-passau.de (Ignaz Rutter)

1 Introduction

We study whether a clustered planar graph $\mathcal{C}$ has a planar straight-line drawing on a prescribed set of disks where each edge is allowed to intersect the boundary of each disk at most once. More formally, a *(flat) clustering* of a graph $G = (V, E)$ is a partition $\mathcal{V} = \{V_1, \ldots, V_k\}$ of the vertex set V. We refer to the pair $\mathcal{C} = (G, \mathcal{V})$ as a *clustered graph* and the graphs $G_i = (V_i, E_i)$ induced by V_i as *clusters*. The set of edges E_i of a cluster G_i are *intra-cluster edges* and the set of edges with endpoints in different clusters are *inter-cluster edges*. A *disk arrangement* $\mathcal{D}_\mathcal{C} = \{D_1, \ldots, D_k\}$ *of* $\mathcal{C}$ is a set of disks in the plane together with a bijective mapping $\mu(V_i) = D_i$ between the clusters $\mathcal{V}$ and the disks $\mathcal{D}$.

A *pipe* p_{ij} *of two clusters* V_i, V_j is the *convex hull* of the disks D_i and D_j, i.e., the smallest convex set of points containing D_i and D_j; see Figure 1. Observe that the boundary of p_{ij} is composed of two line segments u_{ij}, b_{ij} and two circular arcs. We refer to a *topological* planar drawing of G, i.e., the drawing of each edge is a curve, as an *embedding of* G. A $\mathcal{D}_\mathcal{C}$*-framed embedding of* G is an embedding of G where each vertex $v \in V_i$ lies in the interior of the disk D_i and each edge uv, with $u \in V_i$ and $v \in V_j$, lies entirely in the pipe of V_i and V_j.

Given a cluster planar graph $\mathcal{C}$, a disk arrangement $\mathcal{D}_\mathcal{C}$ of $\mathcal{C}$ and a $\mathcal{D}_\mathcal{C}$-framed embedding ψ, Godau [11] proves that it is $\mathcal{NP}$-hard to decide whether G has a $\mathcal{D}_\mathcal{C}$-framed straight-line drawing Γ such that ψ is homeomorphic to Γ. The gadgets in the proof contain disks of size 0, i.e., the positions of some vertices are fixed. Moreover, there are disks that are entirely contained in a larger disk, i.e., there exist two disk $d_i, d_j, i \neq j$ with $d_i \subset d_j$. Angelini et al. [4] consider the case where G is not embedded but all disks have unit size. More formally, they show that given a planar graph G, it is $\mathcal{NP}$-hard to decide whether G has a $\mathcal{D}_\mathcal{C}$-framed straight-line drawing. For unit disks, they leave the computational complexity of the question whether a $\mathcal{D}_\mathcal{C}$-framed embedding has a corresponding $\mathcal{D}_\mathcal{C}$-framed straight-line drawing as an open question. Banyassady et al. [6] show that this problem is $\mathcal{NP}$-hard in case that G is the *intersection graph* of $\mathcal{D}_\mathcal{C}$, i.e., each vertex corresponds to a disk and two vertices are joined by an edge if the intersection of the corresponding disks is not empty.

The computational complexity of the following problem has not been considered: Given a cluster planar graph $\mathcal{C} = (G, \mathcal{V})$, a set of pairwise disjoint disks $\mathcal{D}$ and a $\mathcal{D}_\mathcal{C}$-framed embedding ψ, does $\mathcal{C}$ admit a $\mathcal{D}_\mathcal{C}$-framed straight-line drawing of $\mathcal{C}$ that is *homeomorphic* to ψ. Thereby, we consider two $\mathcal{D}_\mathcal{C}$-framed embeddings ψ, ψ' of $\mathcal{C}$ to be *homeomorphic* if (i) ψ and ψ' have the same combinatorial embedding and the same outer face, (ii) each edge e of G crosses a line segment u_{ij} (b_{ij}) of a pipe p_{ij} in ψ if and only if it crosses the respective line segment in ψ', (iii) and it does so in the same order. Observe that every edge in a $\mathcal{D}_\mathcal{C}$-framed straight-line drawing intersects the boundary of a pipe at most twice; see Figure 1. Thus, in the following we assume as a necessary condition that an edge in a $\mathcal{D}_\mathcal{C}$-framed embedding crosses the boundary of a pipe at most twice.

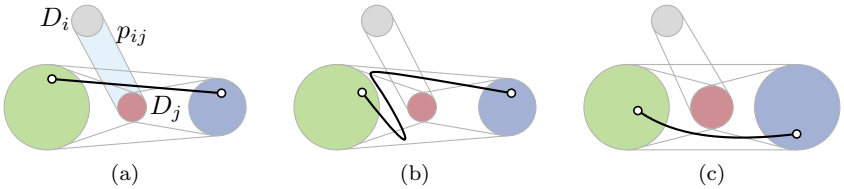

Figure 1: (a) The light-blue region shows the pipe p_{ij} of the disks D_i and D_j. An edge in a $\mathcal{D}_\mathcal{C}$-framed straight-line drawing intersects the boundary of a pipe at most two times. Thus, the $\mathcal{D}_\mathcal{C}$-framed embedding described in (b) does not correspond to $\mathcal{D}_\mathcal{C}$-framed straight-line drawing. The drawing in (c) is not homeomorphic to (a), since the edge in (c) intersects different parts of the boundaries of the pipes.

Related Work Feng et al. [10] introduced the notion of *clustered graphs* and *c-planarity*. A graph G together with a recursive partitioning of the vertex set is considered to be a clustered graph. An embedding of G is *c-planar* if (i) each cluster c is drawn within a connected region R_c, (ii) two regions R_c, R_d intersect if and only if the cluster c contains the cluster d or vice versa, and (iii) every edge intersects the boundary of a region at most once. They prove that a c-planar embedding of a connected clustered graph can be computed in $O(n^2)$ time. It is an open question whether this result can be extended to disconnected clustered graphs. Many special cases of this problem have been considered [7].

Eades et al. [9] prove that every c-planar graph has a c-planar straight-line drawing where each cluster is drawn in a convex region. Angelini et al. [5] strengthen this result by showing that every c-planar graph has a c-planar straight-line drawing in which every cluster is drawn in an axis-parallel rectangle. The result of Akitaya et al. [2] implies that in $O(n \log n)$ time one can decide whether an abstract graph with a flat clustering has an embedding where each vertex lies in a prescribed topological disk and every edge is routed through a prescribed topological pipe. In general they ask whether a simplicial map φ of G onto a 2-manifold M is a *weak embedding*, i.e., for every $\epsilon > 0$, φ can be perturbed into an embedding ψ_ϵ with $||\varphi - \psi_\epsilon|| < \epsilon$.

Alam et al. [3] prove that it is $\mathcal{NP}$-hard to decide whether an embedded clustered graph has a c-planar straight-line drawing where every cluster is contained in a prescribed (thin) rectangle and edges have to pass through the interval common for both rectangles. Further, they prove that all instances with biconnected clusters always admit a solution. Their result implies that graphs of this class have $\mathcal{D}_\mathcal{C}$-framed straight-line drawings.

Ribó [13] shows that every embedded clustered graph where each cluster is a set of independent vertices has a straight-line drawing such that every cluster lies in a prescribed disk. In contrast to our setting Ribó allows an edge e to intersect a disk of a cluster G_i that does not contain an endpoint of e.

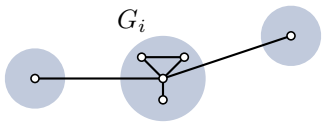

Figure 2: The cluster G_i cannot be augmented with edges such that G_i becomes biconnected.

Contribution We say that a disk arrangement $\mathcal{D}_\mathcal{C}$ is *pipe-disk intersection free* if each pipe p_{ij} that contains an edge (i.e, $(V_i \times V_j) \cap E \neq \emptyset$) does not have an intersection with a disk d_k, where $k \neq i, j$. In Section 2, we prove that if the disk arrangement $\mathcal{D}_\mathcal{C}$ is pipe-disk intersection free and each pair of disks is disjoint, then every clustered planar graph $(G, \mathcal{V})$ with a $\mathcal{D}_\mathcal{C}$-framed embedding ψ has a $\mathcal{D}_\mathcal{C}$-framed planar straight-line drawing homeomorphic to ψ. Taking the result of Akitaya et al. [2] into account, our result can be used to test whether an abstract clustered graph with connected clusters has a $\mathcal{D}_\mathcal{C}$-framed straight-line drawing. The example in Figure 2 shows that in general clusters cannot be augmented to be biconnected, if the embedding is fixed. Hence, our result is generalization of the result of Alam et al. [3]. In Section 3, we show that the problem is $\mathcal{NP}$-hard in the case that the disk arrangements is not pipe-disk intersection free. More specifically, we show that the problem is $\mathcal{NP}$-hard in case of arrangements of unit disks and as well as in the case of axis-aligned unit squares. This answers the aforementioned open question of Angelini et al. [4]. From now on we refer to a $\mathcal{D}_\mathcal{C}$-framed straight-line drawing of G simply as a *$\mathcal{D}_\mathcal{C}$-framed drawing* of G.

2 Drawing on Disk Arrangements that are Pipe-Disk Intersection Free

Let $\mathcal{C} = (G, \mathcal{V})$ be a clustered planar graph, let $\mathcal{D}_\mathcal{C}$ be a disk arrangement with pairwise disjoint disks that is pipe-disk intersection free, and let ψ be a $\mathcal{D}_\mathcal{C}$-framed embedding of $\mathcal{C}$. In this section we prove that $\mathcal{C}$ has a $\mathcal{D}_\mathcal{C}$-framed drawing that is homeomorphic to ψ. We prove the statement by induction on the number of intra-cluster edges. In Lemma 1 we show that we can indeed reduce the number of intra-cluster edges by contracting intra-cluster edges. In Lemma 2, we prove that the statement is correct if the outer face of $\mathcal{C}$ is a triangle and $\mathcal{C}$ is *connected*, i.e., each cluster G_i is connected. In Theorem 1 we extend this result to clustered graphs whose clusters are not connected.

A triangle T in an embedded planar graph G is *separating* if the interior and exterior of T each contain a vertex of G. Let $e = uv$ be an intra-cluster edge of G that is not an edge of a separating triangle. We obtain a *contracted clustered graph* $\mathcal{C}/e$ of $\mathcal{C}$ by removing v from G and connecting the neighbors of v to u. We obtain a corresponding embedding ψ/e from ψ by routing the edges $vw \in E, w \neq u$ close to the original drawing of uv.

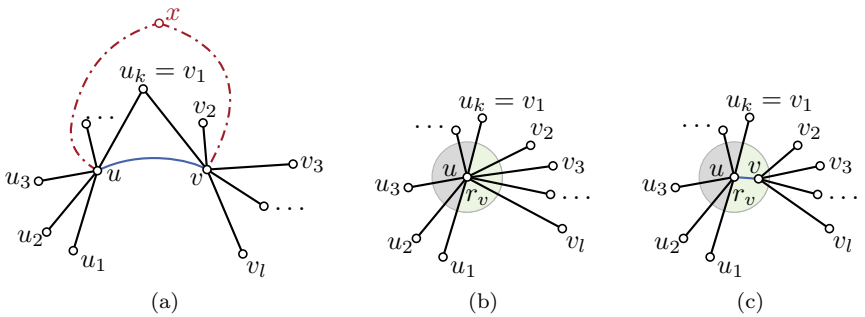

Figure 3: (a) Since uv is not an edge of a separating triangle edges xu, xv do not exist. (b) Moving u within disk d_u preserves the embedding of G/uv. (c) Drawing of G obtained from (b) by placing v in r_v.

Lemma 1 *Let $\mathcal{C} = (G, \mathcal{V})$ be a connected clustered planar graph, $\mathcal{D}_\mathcal{C}$ be a disk arrangement with pairwise disjoint disks that is pipe-disk intersection free and let ψ be $\mathcal{D}_\mathcal{C}$-framed embedding of $\mathcal{C}$. Let e be an intra-cluster edge that is not an edge of a separating triangle. Then $\mathcal{C}$ has a $\mathcal{D}_\mathcal{C}$-framed drawing that is homeomorphic to ψ if $\mathcal{C}/e$ has a $\mathcal{D}_\mathcal{C}$-framed drawing that is homeomorphic to ψ/e.*

Proof: Let $e = uv$ and denote by $u_0, u_1, \ldots, u_k$ the neighbors of u and denote by $v_0, v_1, \ldots, v_l$ the neighbors of v in $\mathcal{C}$ in clockwise order; see Figure 3a. Without loss of generality, we assume that $u_0 = v$ and $v_0 = u$. Since e is not an edge of a separating triangle the set $I := \{u_2, \ldots, u_{k-1}\} \cap \{v_2, \ldots, v_{l-1}\}$ is empty. Denote by u the vertex obtained by the contraction of e. Let G_i be the cluster of u and v, and let D_i be the corresponding disk in $\mathcal{D}_\mathcal{C}$.

Consider a $\mathcal{D}_\mathcal{C}$-framed drawing Γ/e of $\mathcal{C}/e$ homeomorphic to ψ/e; see Figure 3b. Then there is a small disk $D_u \subset D_i$ around u such that for every point p in D_u moving u to p yields a $\mathcal{D}_\mathcal{C}$-framed drawing that is homeomorphic to ψ/e.

We obtain a straight-line drawing Γ of $\mathcal{C}$ from Γ/e as follows; see Figure 3c. First, we remove the edges uv_i from Γ/e. The edges uu_1, uu_k partition D_u into two regions r_u, r_v such that the intersection of r_v with uu_i is empty for all $i \in \{2, \ldots, k-1\}$. We place v in r_v and connect it to u and the vertices $v_1, \ldots, v_l$. Since r_v is a subset of D_u and $I = \emptyset$, we have that the new drawing Γ is planar. Since v is placed in r_v, the edge uv is in between uu_1 and uu_k in the rotational order of edges around u. Hence, Γ is homeomorphic to ψ. Finally, Γ is a $\mathcal{D}_\mathcal{C}$-framed drawing since, D_u is entirely contained in D_i and thus are u and v. □

Lemma 2 *Let $\mathcal{C}$ be a connected clustered graph with a triangular outer face T, let $\mathcal{D}_\mathcal{C}$ be a disk arrangement with pairwise disjoint disks that is pipe-disk intersection free, and let ψ be a $\mathcal{D}_\mathcal{C}$-framed embedding of $\mathcal{C}$. Moreover, let Γ_T be a $\mathcal{D}_\mathcal{C}$-framed drawing of T. Then $\mathcal{C}$ has a $\mathcal{D}_\mathcal{C}$-framed drawing that is homeomorphic to ψ with the outer face drawn as Γ_T.*

Proof: We prove the theorem by induction on the number of intra-cluster edges.

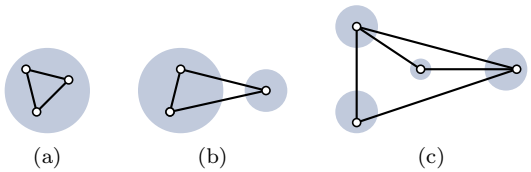

Figure 4: Instances with a triangular outer face that do not contain contractable intra-cluster edges.

First, consider the case that every intra-cluster edge of $\mathcal{C}$ is an edge on the boundary of the outer face. Note that there are at most three vertices in the interior of a single disk. Thus, $\mathcal{C}$ is either a triangle as depicted in Figure 4a and Figure 4b, or each cluster is a single vertex. Since $\mathcal{D}_\mathcal{C}$ is pipe-disk intersection free, the graph in Figure 4a and Figure 4b $\mathcal{C}$ does not contain any further vertices. Let Γ be the drawing obtained from Γ_T by placing every vertex that does not lie on the outer face on the center point of its corresponding disk. Since $\mathcal{D}_\mathcal{C}$ is a pipe-disk intersection free and Γ_T is convex, the resulting drawing is planar and thus a $\mathcal{D}_\mathcal{C}$-framed drawing of $\mathcal{C}$ that is homeomorphic to the embedding ψ.

Let S be a separating triangle of $\mathcal{C}$ that splits $\mathcal{C}$ into two subgraphs $\mathcal{C}_{\text{in}}$ and $\mathcal{C}_{\text{out}}$ so that $\mathcal{C}_{\text{in}} \cap \mathcal{C}_{\text{out}} = S$ and the outer face of $\mathcal{C}_{\text{out}}$ and $\mathcal{C}$ coincide. Note that $\mathcal{C}_{\text{in}}$ and $\mathcal{C}_{\text{out}}$ are connected as otherwise $\mathcal{C}$ itself would not be connected. Then by the induction hypothesis $\mathcal{C}_{\text{out}}$ has the $\mathcal{D}_\mathcal{C}$-framed drawing Γ_{out} with the outer face drawn as Γ_T and $\mathcal{C}_{\text{in}}$ has a $\mathcal{D}_\mathcal{C}$-framed drawing Γ_{in} with the outer face drawn as $\Gamma_{\text{out}}[S]$, where $\Gamma_{\text{out}}[S]$ is the drawing of S in Γ_{out}. Then we obtain a $\mathcal{D}_\mathcal{C}$-framed drawing of $\mathcal{C}$ by merging Γ_{in} and Γ_{out}.

Consider an intra-cluster edge e that does not lie on the boundary of the outer face and is not an edge of a separating triangle. Then by the induction hypothesis, $\mathcal{C}/e$ has a $\mathcal{D}_\mathcal{C}$-framed drawing with the outer face drawn as Γ_T. It follows by Lemma 1 that $\mathcal{C}$ has a $\mathcal{D}_\mathcal{C}$-framed drawing homeomorphic to ψ. □

Theorem 1 *Every clustered graph $\mathcal{C}$ with a $\mathcal{D}_\mathcal{C}$-framed embedding ψ has a $\mathcal{D}_\mathcal{C}$-framed drawing homeomorphic to ψ if the disk arrangement $\mathcal{D}_\mathcal{C}$ is pairwise disjoint and pipe-disk intersection free.*

Proof: We obtain a clustered graph $\mathcal{C}'$ from $\mathcal{C}$ by adding a new triangle T to the graph and assigning each vertex of T to a newly constructed cluster. Let Γ_T be a drawing of T that contains all disks in $\mathcal{D}_\mathcal{C}$ in its interior. We obtain a new disk arrangement $\mathcal{D}'_\mathcal{C}$ from $\mathcal{D}_\mathcal{C}$ by adding a sufficiently small disk for each vertex of Γ_T. The embedding ψ together with Γ_T is a $\mathcal{D}'_\mathcal{C}$-framed embedding ψ' of $\mathcal{C}'$.

According to Feng et al. [10] there is a simple connected clustered graph $\mathcal{C}''$ that contains $\mathcal{C}'$ as a subgraph whose embedding ψ'' is $\mathcal{D}_\mathcal{C}$-framed and contains ψ'. By Lemma 2 there is a $\mathcal{D}_\mathcal{C}$-framed drawing Γ'' of $\mathcal{C}''$ homeomorphic to ψ''

with the outer face drawn as Γ_T. The drawing Γ'' contains a $\mathcal{D}_\mathcal{C}$-framed drawing of $\mathcal{C}$. □

3 Drawing on Arrangements with Pipe-Disk Intersections

In this section we study the following problem referred to as $\mathcal{D}_\mathcal{C}$-FRAMED DRAWINGS WITH PIPE-DISK INTERSECTIONS. Given a planar clustered graph $\mathcal{C} = (G, \mathcal{V})$, a disk arrangement $\mathcal{D}_\mathcal{C}$ with pairwise disjoint disks that is not disk-pipe intersection free, and a $\mathcal{D}_\mathcal{C}$-framed embedding ψ of $\mathcal{C}$, is there a $\mathcal{D}_\mathcal{C}$-framed drawing Γ that is homeomorphic to ψ?

Note that if the disks $\mathcal{D}_\mathcal{C}$ are allowed to overlap and G is the intersection graph of $\mathcal{D}_\mathcal{C}$, the problem is known to be $\mathcal{NP}$-hard [6]. Thus, in the following we require that the disks do not overlap, but there can be pipe-disk intersections. By Alam at al. [3] it follows that the problem restricted to thin touching rectangles instead of disks is $\mathcal{NP}$-hard. Their reduction heavily relies on the fact that the rectangles are thin. We strengthen this result and prove that in case that the rectangles are either axis-aligned unit squares or unit disks and are not allowed to touch the problem remains $\mathcal{NP}$-hard.

To prove $\mathcal{NP}$-hardness we reduce from PLANAR MONOTONE 3-SAT [8]. For each literal and clause we construct a clustered graph $\mathcal{C}$ with an arrangement of disks (squares) $\mathcal{D}_\mathcal{C}$ of $\mathcal{C}$ such that each disk (square) contains exactly one vertex. We refer to these instances as *literal* and *clause gadgets*. In order to transport information from the literals to the clauses, we construct a *copy* and *inverter gadget*. For each gadget we first construct an arrangement of unit squares and state its important properties in this case. This is followed by the corresponding arrangement of unit disks. We emphasize the differences that have to be dealt with to preserve the properties of the gadgets when considering unit disks instead of unit squares. The design of the gadgets is inspired by Alam et al. [3], but the restriction to unit disks and squares rather than thin touching rectangles, requires a more complex construction and a careful placement of the geometric objects. The green and red regions in the figures of the gadget correspond to *positive* and *negative* drawings of the literal gadget. The green and red line segments indicate that for each truth assignment of the variables our gadgets indeed have $\mathcal{D}_\mathcal{C}$-framed straight-line drawings. Negative versions of the literal and clause gadget are obtained by mirroring vertically. Hence, we assume that variables and clauses are positive. Each gadget covers a set of checkerboard cells. This simplifies the assembly of the gadgets in the final reduction. Note that in the following constructions all squares and disks will be of unit size. Moreover, we consider only axis-aligned squares.

3.1 Regulator

A line l separates the euclidean plane in two *half planes* h_a *and* h_b and we denote by $\overline{h_a}$ the complement of h_a. These half planes are *spanned by* l. We

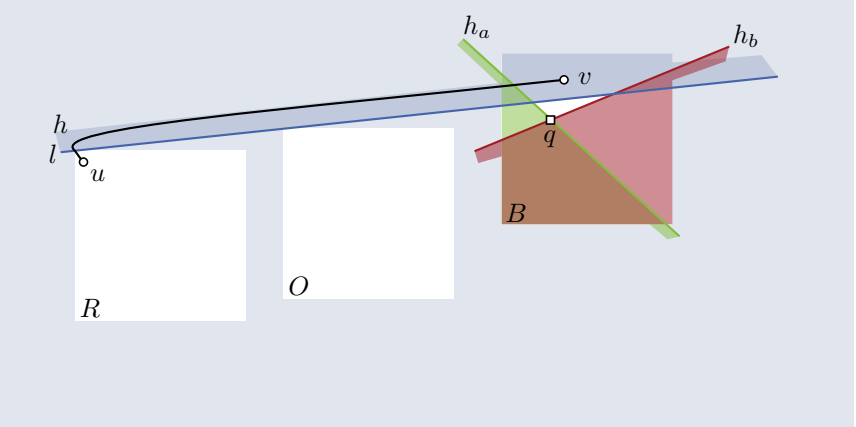

Figure 5: Regulator gadget

say that l *supports* h_a *(*h_b*).* Let B be an axis-aligned square that contains a vertex v in its interior and let h_a, h_b be two half planes whose supporting lines have a unique intersection point q that lies in the interior of B; see Figure 5. We describe the construction of a gadget that restricts the feasible placements of v in a $\mathcal{D}_\mathcal{C}$-framed drawing by a half plane h that excludes a placement of v in $h_a \cap h_b$ but allows for a placement in $h_a \cap B$ or $h_b \cap B$. Since q lies in the interior of B, there is a half plane h that does not contain q and for each $i = a, b$, $h \cap h_i \cap B$ is not empty, but $h \cap h_a \cap h_b = \emptyset$.

Let h, h_a, h_b and B as described before. We construct a *regulator gadget of* v *in* B *with respect to* h_a *and* h_b as follows. Let l_h be the supporting line of h. We create two axis-aligned squares R and O such that R, O and B intersect l_h in this order and h neither intersects the interior of R nor the interior of O. Place a vertex u in R and route an edge uv through $h \cup R \cup B$. In case that h instead of h_a and h_b is given, we refer to the gadget as the *regulator of* v *with respect to a (single) half plane* h.

Lemma 3 *Let* W *be a regulator gadget of* v *in* B *with respect to* h_a *and* h_b*. For every point* $p_v \in h \cap B$ *there is a* $\mathcal{D}_\mathcal{C}$*-framed drawing* Γ *such that* v *lies on* p_v*. There is no* $\mathcal{D}_\mathcal{C}$*-framed drawing of* W *such that* v *lies in* $\overline{h} \cap B$*.*

Proof: By construction of W, there is for every point $p_v \in h \cap B$ a $\mathcal{D}_\mathcal{C}$-framed drawing Γ such that v lies on p_v.

The supporting line l_h of h intersects the boundary of R and does not intersect the interior of O. Let r and o be points in the intersection of l_h with R and O, respectively. Since Γ is homeomorphic to W the edge uv intersects l_h on the ray starting in o in the direction towards r. Therefore, u and v lie on different sides of l_h. Since $u \in R$, it follows that $v \in \overline{h}$. □

We refer to the intersection $h \cap B$ as the *regulated region of* v *in* B. Thus, by the construction of W, the regulated region Q has a non-empty intersection

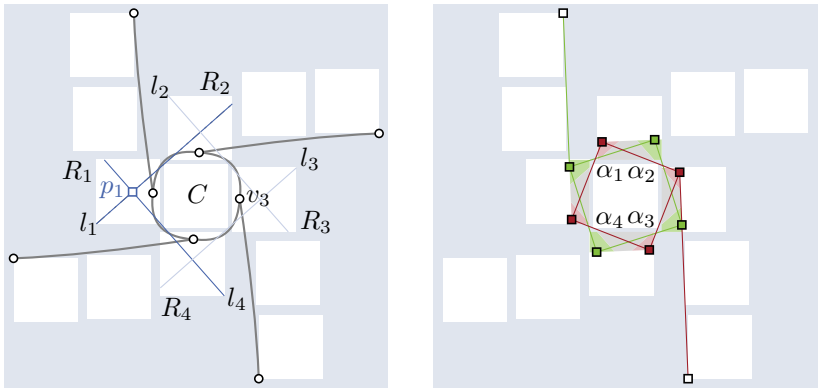

(a) (b)

Figure 6: (a) The literal gadget. (b) The positive regions P_i are depicted in green and the negative regions N_i are red. The grey regions Q_i are infeasible. The green / red squared indicate that there are positive and negative realizations of the literal gadget.

with $h_a \cap B$ and $h_b \cap B$. Thus, by the lemma for each placement of v in $Q \cap h_i \cap B, i = a, b$, there is a $\mathcal{D}_\mathcal{C}$-framed drawing. On the other hand, since $h \cap h_a \cap h_b \cap B = \emptyset$, there is no $\mathcal{D}_\mathcal{C}$-framed drawing such that v lies in $h_a \cap h_b \cap B$.

3.2 Literal Gadget

In this section we construct a clustered graph $\mathcal{C}$ with an arrangement of squares $\mathcal{D}_\mathcal{C}$ that models a literal u. The *positive literal gadget* is depicted in Figure 6a. We obtain the *negative literal gadget* by mirroring vertically.

The *center block* is a unit square C with corners $\alpha_1, \alpha_2, \alpha_3, \alpha_4$ in clockwise order. For each corner α_i of C consider a line l_i that is tangent to C in α_i, i.e, $l_i \cap C = \{\alpha_i\}$. Let p_i be the intersection of the lines l_{i-1} and l_i where $l_0 = l_4$; refer to Figure 6a. Let $R_1, \ldots, R_4$ be four pairwise non-intersecting squares that are disjoint from C such that R_i contains p_i in its interior. We add a cycle $v_1 v_2 v_3 v_4 v_1$ to the graph such that $v_i \in R_i$. We refer to the vertex v_i as the *cycle vertex* of the *cycle block* R_i. For each i, let η_i be a half plane that contains R_{i+1} but does not intersect C. Within η_i we place a regulator W_i of v_i with respect to h_{i-1} and h_i, where h_i is the half plane spanned by l_i that does not contain C. This finishes the construction.

We now show that there exist two disjoint regions P_i and N_i in R_i that correspond to a positive and negative drawing of the literal gadget. Consider R_1 and its two adjacent squares R_4 and R_2. Let Q_i be the regulated region of R_i with respect to W_i. Then the intersection $I_1 := \overline{h_4} \cap \overline{h_1} \cap Q_1 \neq \emptyset$. We refer to I_1 as the *infeasible region of* R_1. The intersection $h_1 \cap Q_1$ is the *positive region* P_1 *of* R_1. The region $h_4 \cap Q_1$ is the *negative region* N_1 *of* R_1. Regions

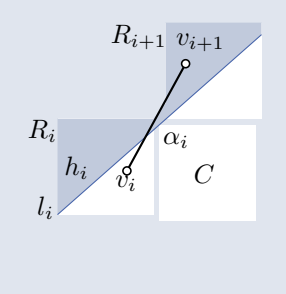

Figure 7: Since v_i does not lie in $h_i \cap R_i$ (green) and l_i is tangent to C, v_{i+1} lies in the $h_{i+1} \cap R_{i+1}$ (red).

P_1, N_1, I_1 are by construction not empty. The positive, negative and infeasible region of $R_i, i \neq 1$ are defined analogously.

Property 2 *If Γ is a $\mathcal{D}_\mathcal{C}$-framed drawing of a literal gadget, then no cycle vertex v_i lies in the infeasible region of R_i. Moreover, either each cycle vertex v_i lies in the positive region P_i or each vertex v_i lies in the negative region N_i.*

Proof: Consider a $\mathcal{D}_\mathcal{C}$-framed drawing Γ with an edge v_iv_{i+1} such that v_i lies in $\overline{P_i}$, i.e., v_i lies in $\overline{h_i} \cap R_i$; see Figure7. We show that v_{i+1} lies in N_{i+1}. If v_{i+1} lies in $\overline{h_i}$, then v_i and v_{i+1} lie on the same side of l_i. Since l_i is tangent to α_i, v_iv_{i+1} intersects C. It follows that v_{i+1} lies in h_i and therefore in the negative region N_{i+1}.

Assume that v_1 lies in its infeasible region I_1, then v_2 lies in N_2 by the above observation. Likewise, v_3, v_4, v_1 lie in N_3, N_4, N_1, respectively. This contradicts $N_1 \cap I_1 = \emptyset$. Similarly, we get that each vertex $v_i, i \neq 1$, cannot lie in the invisible region I_i. Thus, each v_i either lies in P_i or in N_i. Moreover, if one v_i lies in N_i the above observation yields that all of them lie in their negative region. □

The green and red squares in Figure 6a indicate that there is a positive and a negative realization of the literal gadget, i.e., there is a $\mathcal{D}_\mathcal{C}$-framed drawing of the literal gadget where all cycle vertices lie either in a positive or in a negative region. In order to simplify the following constructions, we fix the position of the green and red squares as depicted. We refer to these positions as the *positive and negative placement* of the vertices v_i and denote them by $p^+_{X,i}$ and $p^-_{X,i}$. To reduce the notation, we drop the index i and simply refer to p^+_X and p^-_X as the positive and negative placements of the literal X. Thus, the literal gadget has the following property.

Property 3 *The positive and negative placements induce a $\mathcal{D}_\mathcal{C}$-framed drawing of the literal gadget, respectively.*

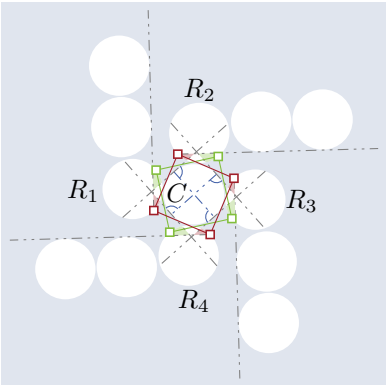

Figure 8: The literal gadget with unit disks. The endpoints of the blue segment in the interior of the central disk C are the points β_i.

Unit Disks

The construction of the literal gadget with unit disks follows the same principle as the construction using unit squares; see Figure 8. Only instead of the four corners α_i we choose four points β_i that are equally distributed along the boundary of the central disk. The position of the disk R_i have to be adjusted so that the it contains the intersection of the tangents of the central disks in the points β_{i-1} and β_i.

3.3 Copy and Inverter Gadget

In this section, we describe the copy and inverter gadget; see Figure 9. The copy gadget connects two positive or two negative literal gadgets X and Y such that a drawing of X is positive if and only if the drawing of Y is positive. Correspondingly, the inverter gadget connects a positive literal gadget X to a negative literal gadget Y such that the drawing of X is positive if and only if the drawing of Y is negative. The construction of the inverter and the copy gadget are symmetric.

Let X and Y be two positive literal gadgets whose center blocks are aligned on the x-axis with a sufficiently large distance. We construct the copy gadget that *connects* X and Y as follows. Let R_X and R_Y be the two cycle blocks of the literal gadgets X and Y, respectively, with minimal distance on the x-axis. For $A \in \{X, Y\}$, let P_A and N_A be the positive and negative regions of R_A. Since P_A and N_A are convex and their intersection is empty, there exists a half plane h_A that contains N_A but not P_A, and vice versa. In a reversed manner, we call h_A a *positive half-plane* h_Z^+ *of* A if it contains the negative region N_A, otherwise it is *negative* and we denote it by h_A^-.

Consider a positive half-plane h_X^+ of X and a negative half-plane h_Y^- of Y; refer to Figure 9a. We create two non-intersecting squares O_X^+ and O_Y^- that are

contained in the intersection of $\overline{h_X^+}$ and $\overline{h_Y^-}$ such that a corner of O_X^+ and O_Y^- lie on the supporting line of h_X^+ and h_Y^-, respectively. Recall that we denote the complement of a half-plane h by $\overline{h}$. Let I be the intersection of the supporting lines of h_X^+ and h_Y^-. We place a square B with a vertex b in interior so that the intersection I lies in the interior of B. Additionally, we add a regulator of b with respect to h_X^+ and h_Y^- to exclude the intersection $h_X^+ \cap h_Y^-$ as feasible placement of b. We route the edges bv_X and bv_Y through $R_X \cup h_X^+ \cup B$ and $R_Y \cup h_Y^- \cup B$ respectively. This construction ensures that in a $\mathcal{D}_\mathcal{C}$-framed drawing a placement of the vertex v_X in the positive region P_X excludes the possibility that the vertex v_Y lies in the negative region N_Y. In order to ensure that v_X cannot lie at the same time in N_X as v_Y in P_Y, we construct a square B' with respect to a negative half-plane h_X^- of X and a positive half-plane h_Y^+ of Y analogously to B. If the distance between X and Y is sufficiently large, we can ensure that the intersection of B and B' is empty. In the construction of the inverter gadget the square B is constructed with respect to h_X^+ and h_Y^+, and B' with respect to h_X^- and h_Y^-. We refer to the corresponding gadgets as *copy* and *inverter gadget*. We say that the copy and inverter gadget *connect* two literals.

Property 4 *Let Γ be a $\mathcal{D}_\mathcal{C}$-framed drawing of two positive (negative) literals gadgets X and Y connected by a copy gadget. Then the $\mathcal{D}_\mathcal{C}$-framed of X in Γ is positive if and only if the $\mathcal{D}_\mathcal{C}$-framed drawing of Y is positive.*

Proof: By Property 2 the vertices v_X and v_Y of X and Y cannot lie in the infeasible regions of X and Y, respectively. Thus, similar to the proof of Lemma 2 we can assume for the sake of contradiction that the vertex b of the block B lies in the intersection of $\overline{h_X^+}$ and $\overline{h_Y^-}$. Thus, vertex v_X lies in the negative region of R_X and v_Y in the positive region of R_Y. But then vertex b' of the block B' lies in h_X^- and h_Y^+. However, this is not possible due to the regulator of b'. □

The same argumentation is applicable to the inverter gadget.

Property 5 *Let Γ be a $\mathcal{D}_\mathcal{C}$-framed drawing of a positive literal gadget X and a negative literal gadget Y connected by an inverter gadget. Then the $\mathcal{D}_\mathcal{C}$-framed drawing of X in Γ is positive if and only if the $\mathcal{D}_\mathcal{C}$-framed drawing of Y is negative.*

The green and red squares in Figure 9b and in Figure 10 indicate that for a positive and a negative placement of X there is $\mathcal{D}_\mathcal{C}$-framed drawing of copy and inverter gadget, respectively. Thus, the copy and inverter gadget have the following property.

Property 6 *The positive (negative) placement of two literals gadgets X, Y induces a $\mathcal{D}_\mathcal{C}$-framed straight-line drawing of a copy [inverter] gadget that connects X and Y.*

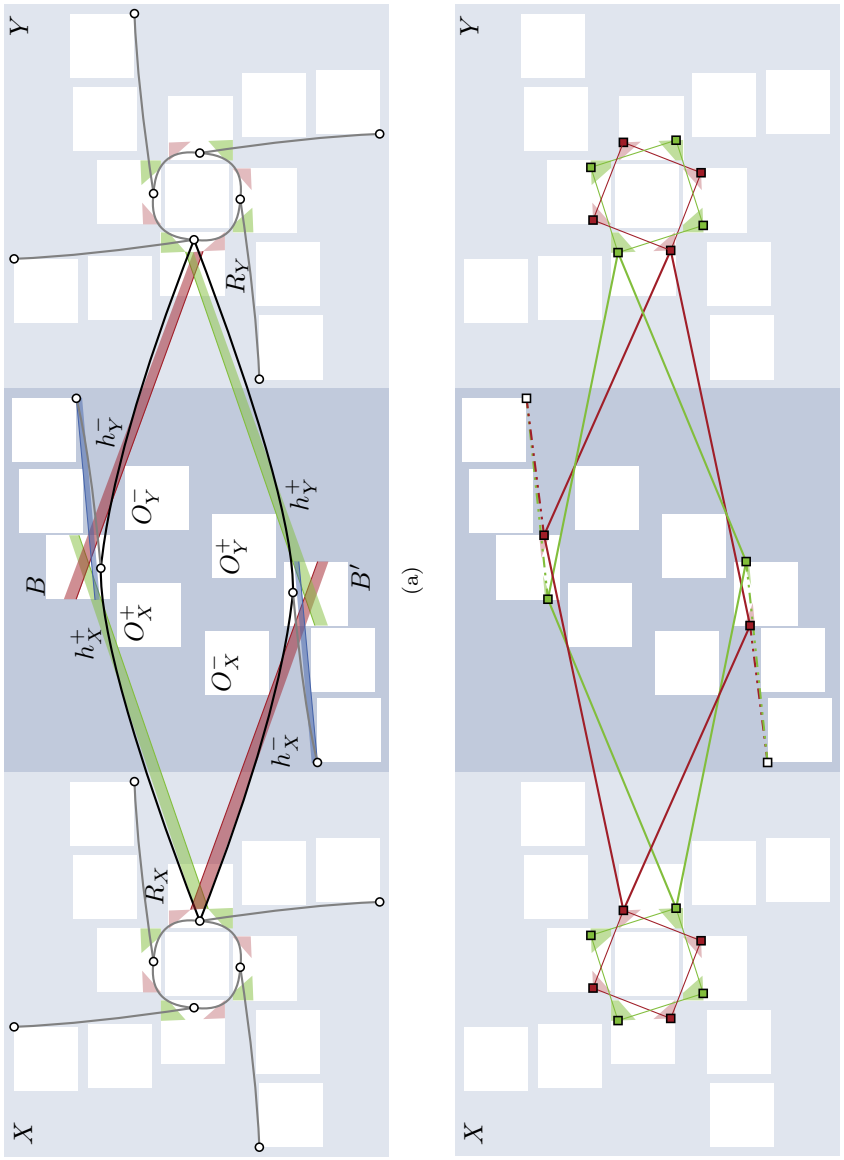

Figure 9: (a) The copy gadget. The thick transparent green and red lines depict the half planes h_X^+, h_Y^+ and h_X^-, h_Y^-, respectively. (b) Green and red regions depict positive and negative regions, respectively.

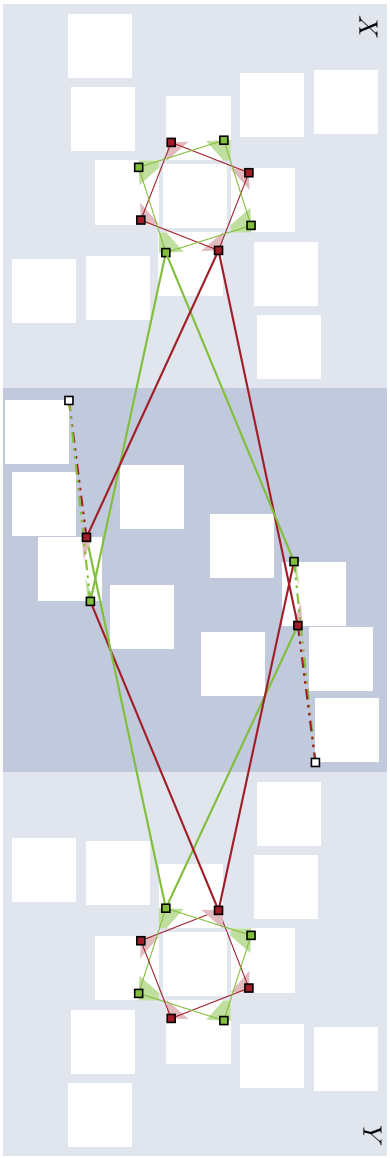

Figure 10: Positive and negative realizations of the inverter gadget.

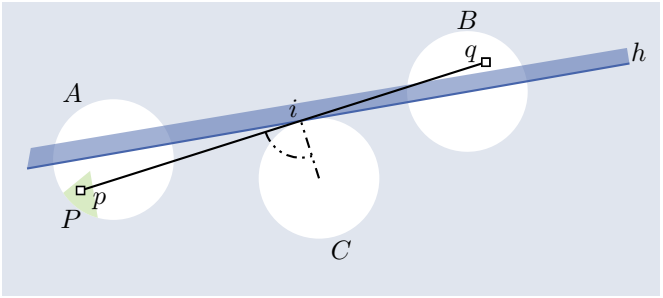

Figure 11: Observation

Unit Disks

Squares have the property that there is a set of tangents through a corner point of the square. On the other hand, at each point on the boundary of a disk the tangent to the disk is unique. The following observation helps to show that this restriction does not invalidate the correctness of the unit-disk gadgets.

Observation 7 *Let A and B be two disks and let P be a non-empty subset of A; see Figure 11. Moreover, let $p \in P$ and $q \in B$. Let i be the intersection of the segment pq and the supporting line of a half plane h that contains q and such that $h \cap P = \emptyset$. Let C be a disk such that pq is tangent to C in the point i. Let Q be the set of points in B so that for each $q' \in Q$ there is a point $p' \in P$ such that the segment $p'q'$ does not intersect C. Then Q is a strict subset of $h \cap B$.*

Recall that, for $A = X, Y$, let p_A^+ and p_A^- be the positive and negative placements of X and Y. Denote by h_A^+ and h_A^- the positive and negative half-planes, respectively, of the disk D_A; see Figure 12. Moreover, let q^+ and q^- be points in $h_X^+ \cap B$ and $h_Y^- \cap B$. Let O_X^+ (O_Y^-) be a disk such that $p_X^+q^+$ ($p_Y^-q^-$) is tangent to O_X^+ (O_Y^-) in intersection of $p_X^+q^+$ ($p_Y^-q^-$) with the supporting line of h_X^+ (h_Y^-). The disks O_X^- and O_Y^+ are positioned accordingly. The regulators of B and B' and Observation 7 ensure X has a positive $\mathcal{D}_\mathcal{C}$-framed drawing if and only if Y has a positive $\mathcal{D}_\mathcal{C}$-framed drawing.

3.4 Clause Gadget

We construct a *clause gadget* with respect to three positive literal gadgets X, Y, Z arranged as depicted in Figure 13. The negative clause gadget, i.e., a clause with three negative literal gadgets, is obtained by mirroring vertically.

We construct the clause gadget in two steps. First, we place a *transition block* T_A close to each literal gadget $A \in \{X, Y, Z\}$. In the second step, we connect the transition block to a vertex k in a *clause block* K such that for every placement of k in K at least one drawing of the literal gadgets has to be positive.

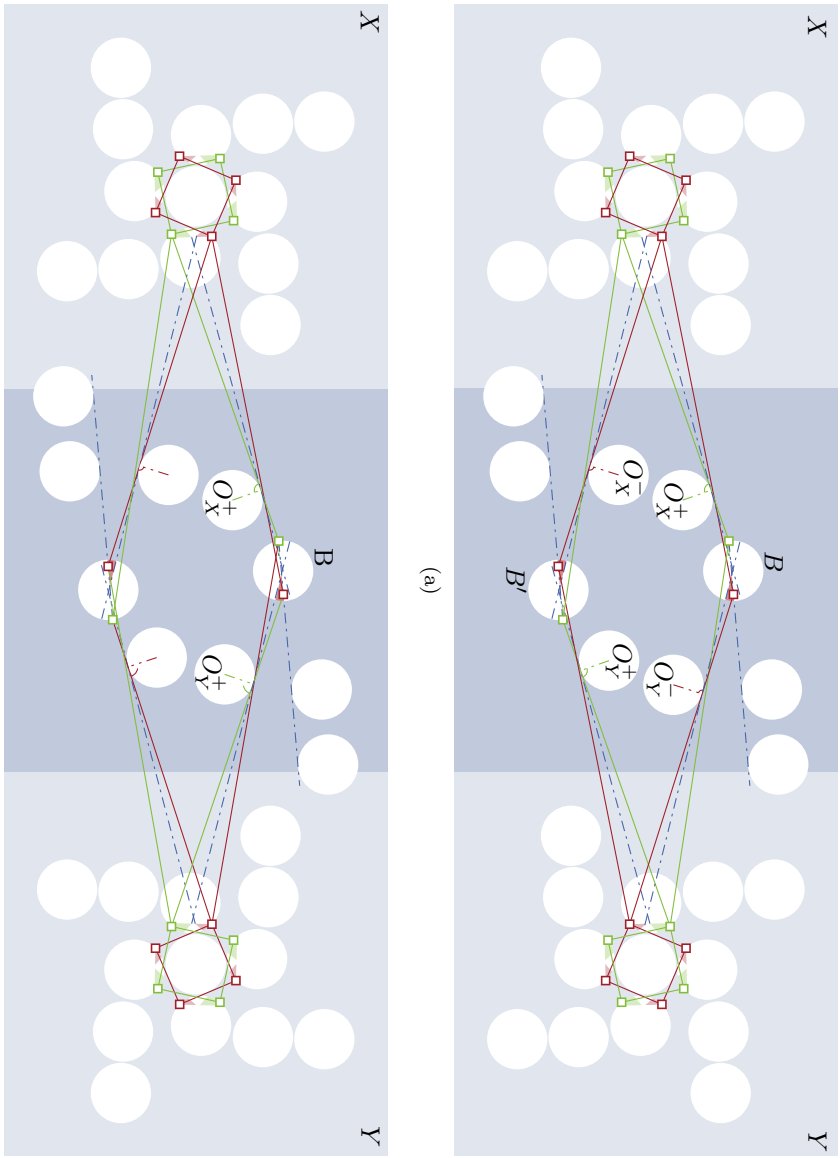

Figure 12: (a) Disk copy gadget. (b) Disk inverter gadget.

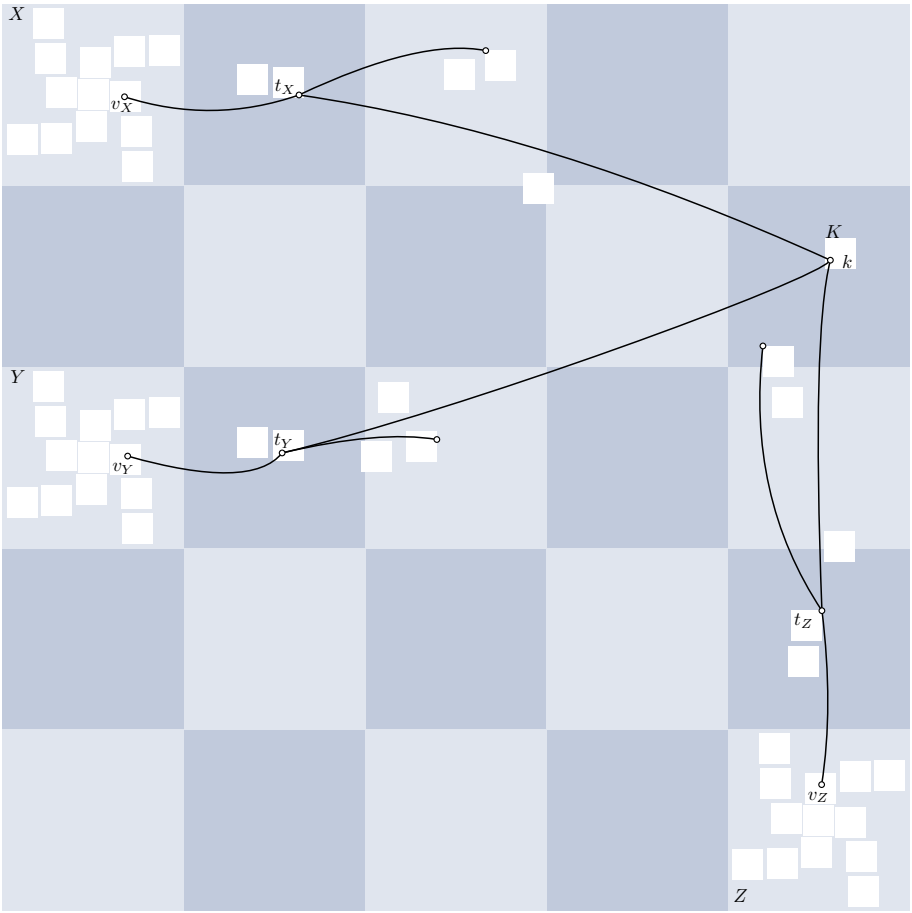

Figure 13: Clause gadget.

Consider the literal gadget X and let R_X be the rightmost cycle block of X. Let h_X^- be a negative half-plane of R_X, i.e., h_X^- contains the positive region but not the negative region; refer to Figure 14. We now place a transition block T_X such that the intersection $T_X \cap h_X^-$ has small area. Recall that p_X^+ and p_X^- denote the positive and negative placements of X, respectively. Let q_X^- be a point in $T_X \cap h_X^-$. Note that, in the following l^- and l^+ denote lines and *not* the half-planes left or right of a line l. Let i be the intersection point of the supporting line l_X^- of h_X^- and the line segment $p_X^- q_X^-$. We place a square Q_X such that l_X^- is tangent to Q_X at point i. We place a *transition vertex* t_X in the interior of T_X and route the edge $v_X t_X$ through $h_X^- \cup T_X \cup R_X$, where $v_X \in R_X$.

Observe that q_X^- allows for a negative drawing of X; see Figure 14. Let l_X^+ be a line that is tangent to Q_X and that contains p_X^+. Then each point on l_X^+ that lies in the interior of T_X allows for a positive drawing of X. Let q_X^+ be the point on l_X^+ that maximizes the distance to q_X^-. We refer to q_X^+ and q_X^- as

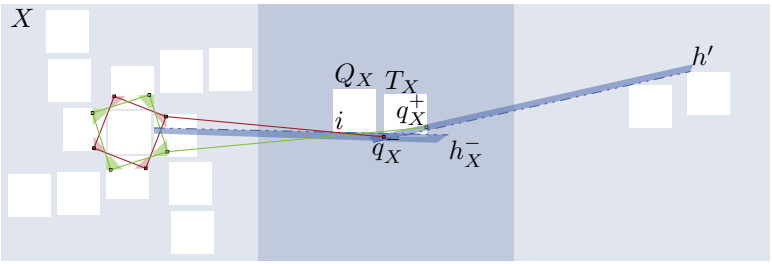

Figure 14: $\mathcal{D}_\mathcal{C}$-framed drawings of the transition block of literal X

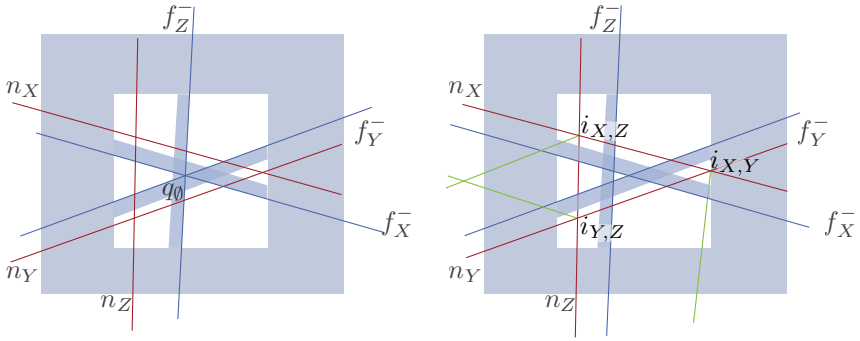

Figure 15: (a) Initial placement of $q_\emptyset$ and the corresponding half planes h_A^-. (b) Setting after perturbing h_A^-. The green segments indicate that each $q_A^+, A = X, Y, Z$ can be connected with a line segment to each intersection $i_{X,Y}, i_{X,Z}, i_{Y,Z}$.

the *positive* and *negative placements of* t_X, respectively. Further, if X has a negative drawing, then t_X lies in the region $h_X^- \cap T_X$. In order to reduce the visibility of t_X in case that X is negative, we place a regulator gadget of T_X with respect to a half plane h' as follows. Let h' be a half plane that contains q_X^- and q_X^+ and reduces the possible positions of t_X in this case to $h' \cap h_X^- \cap T_X$; see Figure 14. In the following, we refer to $h' \cap h_X^- \cap T_X$ as the *negative region* of T_X. The transition blocks of Y and Z are constructed analogously with only minor changes.

Let K be the clause block as depicted in Figure 13. Further, let $q_\emptyset$ be a point in the interior of K. Let f_A^-, for $A \in \{X, Y, Z\}$, be half planes such that the supporting lines of all three half planes intersect at $q_\emptyset$ and such that f_A^- does not contain the negative region N_A of the transition block T_A; see Figure 15. Recall that q_A^- denotes the negative placement of t_A in the transition block T_A. Let n_X and n_Y be two lines whose intersection lies in the interior of $f_X^- \cap f_Y^- \cap K$ and that contain q_X^- and q_Y^-, respectively. Moreover, denote by n_Z a line that

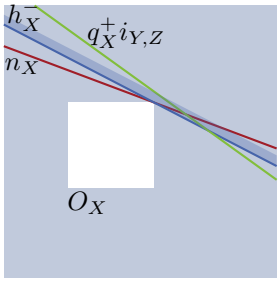

Figure 16: Intersection pattern near square O_X.

contains q_Z^- with a non-empty intersection with $f_Z^- \cap K$. We position a square O_A that is tangent to n_A at point $n_A \cap l_A^-$, where l_A^- is the supporting line of f_A^- and such that the intersection of the interior of O_A and f_A^- is empty. By construction of O_A all three literals gadgets X, Y, Z have negative $\mathcal{D}_\mathcal{C}$-framed drawings if and only if k lies on $q_\emptyset$. Slightly perturbing the positions of the squares O_A ensures that the intersection $f_X^- \cap f_Y^- \cap f_Z^-$ is empty. Denote by $i_{B,C}$, for $B, C \in \{X, Y, Z\}$ with $B \neq C$, the intersection of n_B and n_C. To ensure that there are the necessary positive and negative drawings, the perturbation operation has to ensure that the intersection of the line through q_X^+ and $i_{X,Y}$ with n_B and f_X^- has the pattern as depicted in Figure 16 and correspondingly for the literals Y and Z. Thus, the clause gadget has the following property.

Property 8 *There is no $\mathcal{D}_\mathcal{C}$-framed drawing of the clause gadget such that the $\mathcal{D}_\mathcal{C}$-framed drawing of each literal gadget is negative. For all remaining combinations of positive and negative drawings of the literal gadgets X, Y and Z there is a $\mathcal{D}_\mathcal{C}$-framed drawing of the clause gadget.*

Unit Disks

We utilize Observation 7 twice to ensure the correctness of the clause gadget with unit disks. First, recall that the square Q_X in Figure 14 is positioned such that Q_X is tangent to the supporting line of h_X^- and the line l^- that contains p_X^- and q_X^-, in point i. Replacing Q_X by a disk Q'_X that such that the disk is tangent to l^- in point i ensures that q_X^- corresponds to negative drawing of X. Moreover, by Observation 7 the set of points that possibly allow for a negative drawing is a subset of $h_X^- \cap Q'_X$. The disks Q'_Y, Q'_Z are constructed analogously.

Second, recall the construction of the square O_A for $A = X, Y, Z$. The disk O'_A that corresponds to the square O_A is placed such that the line n_A is tangent to O'_A in the intersection of n_A with the supporting line of the half place f_A^-. Figure 18 shows the final clause gadget with unit disks.

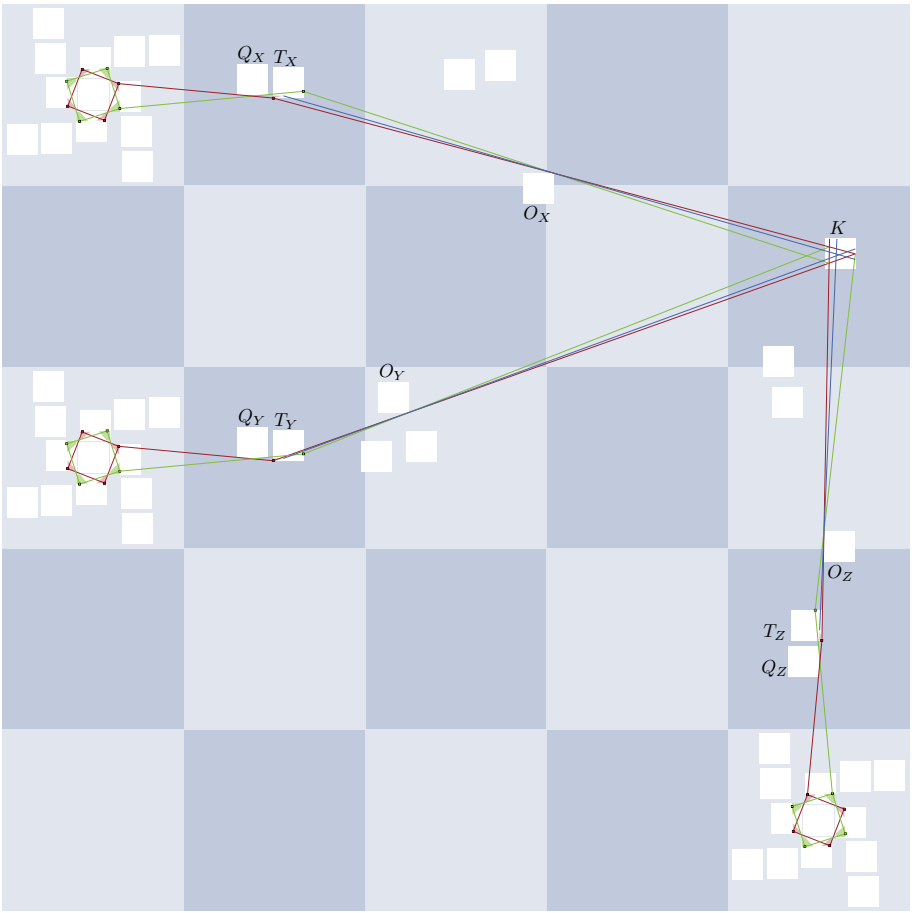

Figure 17: $\mathcal{D}_\mathcal{C}$-framed drawings of the clause gadgets.

3.5 Reduction

A 3-SAT instance (U, C) on a set U of n boolean variables and m clauses C is *monotone* if each clause either contains only positive or only negative literals. It is *planar* if the bipartite graph $G_{U,C} = (U \cup C, \{uc \mid u \in c \text{ or } \overline{u} \in c \text{ with } u \in U \text{ and } c \in C\})$ is planar. A *rectilinear representation* of a monotone planar 3-SAT instance is a drawing of $G_{U,C}$ where each vertex is represented as an axis-aligned rectangle and the edges are vertical line segments touching their endpoints; see Figure 19a. Further, all vertices corresponding to variables lie on a common line l, the positive and negative clauses are separated by l. The problem Monotone Planar 3-SAT asks whether a monotone planar 3-SAT instance with a given rectilinear representation is satisfiable. De Berg and Khosravi [8] proved that Monotone Planar 3-SAT is $\mathcal{NP}$-complete. We use this problem to show that the $\mathcal{D}_\mathcal{C}$-framed Drawings with Pipe-Disk

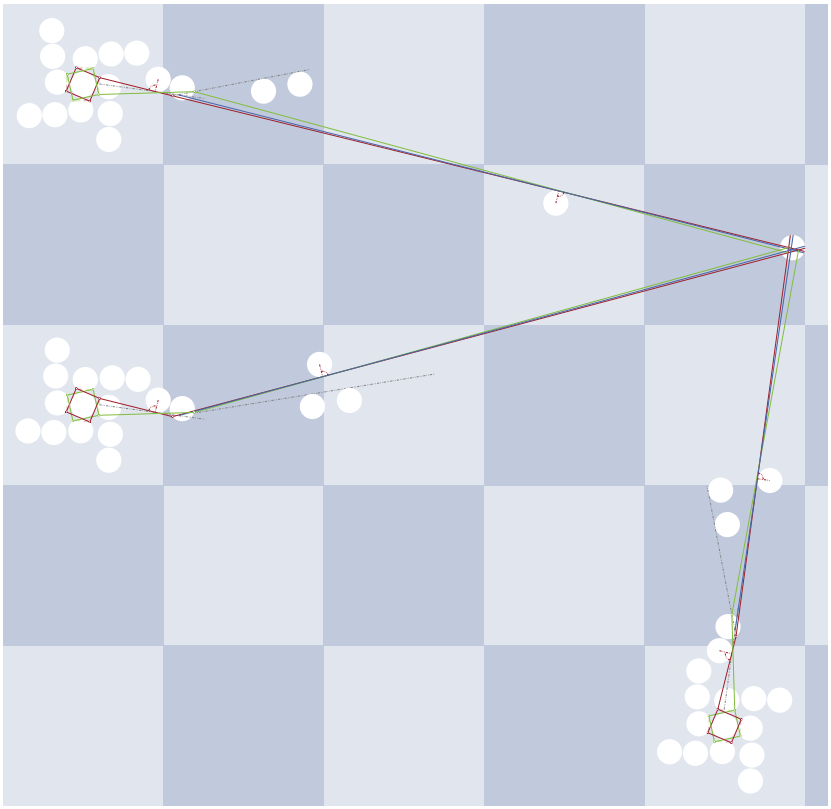

Figure 18: Clause Construction

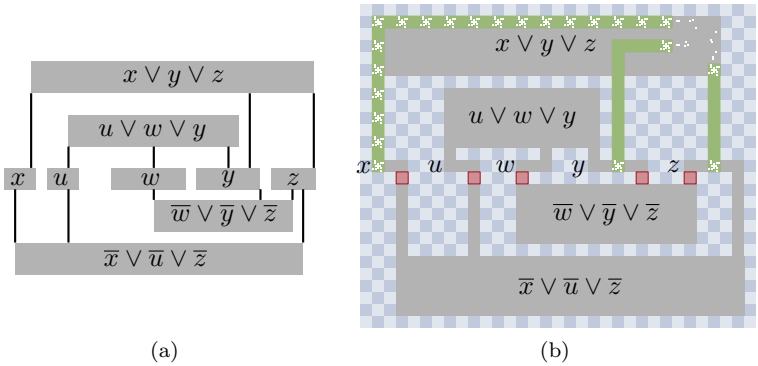

Figure 19: Example of planar monotone 3-SAT instance with a corresponding rectilinear representation.

Intersections problem is $\mathcal{NP}$-hard.

In the following a disk d_k is an *obstacle of a pipe* p_{ij}, for i, j with $i, j \neq k$, if $d_k \cap p_{ij} \neq \emptyset$. The *obstacle number of a pipe* p_{ij} is the number of obstacles of p_{ij}. The *obstacle number of a disk arrangement* $\mathcal{D}_\mathcal{C}$ is the maximum obstacle number over all pipes p_{ij} with $V_i \times V_j \cap E \neq \emptyset$.

Theorem 9 *The problem* $\mathcal{D}_\mathcal{C}$-framed Drawings with Pipe-Disk Intersections *with axis-aligned unit squares and unit disks is* $\mathcal{NP}$*-hard even when the clustered graph* $\mathcal{C}$ *has maximum vertex degree 5 and its obstacle number is* 2.

Proof: Let (U, C) be a planar monotone 3-SAT instance with a rectilinear representation Π. Let l be a horizontal or vertical line that intersects Π. The line l splits Π into two drawings Π_L and Π_R that are left and right of l, respectively. For a positive factor x, we obtain from Π a new rectilinear representation by moving Π_R x units to the right. We fill the resulting gap between Π_L and Π_R with infinitely many copies of $l \cap \Pi$. This operation of *stretching the drawing at line* l allows us to do the following necessary modifications.

In the following we modify Π to fit on a checkerboard of $O(|C|)$ rows and columns where each column has width d and every row has height d. A row or column is *odd* if its index is an odd number, otherwise it is *even*. The pair (i, j) refers to the cell in column i and row j. We align all vertices corresponding to variables in the rectilinear representation in row 0 so that the leftmost variable vertex is in column 1; refer to Figure 19b. The width of each rectangle r_u of variable u is increased to cover $2 \cdot n_u - 1$ columns, where n_u is the number of occurrences of u and $\bar{u}$ in C. To ensure that each r_u starts in an odd column, we increase the distance between two consecutive variables so that the number of columns between the variables is odd and is at least three. Since we are able to add an arbitrary number of columns between two consecutive variables, we can assume without loss of generality that no two edges of the rectilinear representation share a column and that their columns are odd. We adapt the

rectangle of a clause so that it covers five rows and at least six columns, and so that its left and right sides are aligned with the leftmost and rightmost incoming edges, respectively. Note that the positive clauses lie in rows with positive indices and the negative clauses in rows with negative indices. Each operation adds at most a constant number of columns and rows per vertex and per edge to the layout. Thus, the width and height of the final layout is in $O(|C|)$. Further, it can be computed in time polynomial in $|C|$.

In the following we construct a planar embedded graph $\mathcal{C}$ and an arrangement of squares $\mathcal{D}_\mathcal{C}$ of $\mathcal{C}$. We use the modified rectilinear layout to locally replace the variable by a sequence of positive and negative literals connected by either a copy or an inverter gadget. Clauses are replaced with the clause gadget and then connected with a sequence of literals and copy gadget to the respective literal in the variable.

Observe that the literal gadget is constructed so that all its squares fit in a larger square S. The copy and inverter gadget together with two literals is constructed so that they fit in rectangle three times the size of S. The clause gadget fits in a rectangle of width six times the size of the square S and its height is five times the height of S.

We assume that the size of the square S and the size of the squares of the checkerboard coincide. Let $r = 0$ be the row that contains the variable vertices. Every column contains at most one edge of the rectilinear representation. Thus, we place a positive literal gadget in cell (i, r) if the edge in column i connects a variable u to a positive clause. Otherwise, we place a negative literal gadget in cell (i, r). Since every edge of the rectilinear representation lies in an odd column, we can connect two literals of the same variable by either a copy or inverter gadget depending on whether both literals are positive or negative, or one is positive and the other negative.

We substitute an edge e of the rectilinear representation that connects a variable to a positive clause as follows. Let i be the column of e. If the cell (i, r_e) is covered by e and r_e is odd, we place a positive literal gadget in cell (i, r_e). The copy gadget can be rotated in order to connect a literal gadget in cell (i, r_e) to a literal gadget in a cell $(i, r_e + 2)$.

Let R_c be the rectangle that corresponds to the positive clause c in the modified rectilinear representation. We insert a clause gadget in R_c and justify it on the right of it so that the literal gadget Z lies in an odd column. Note that by the construction of clause gadget this fixes the position of the corresponding literal gadgets X and Y. Finally, the literal gadget X, Y and Z can be connected to their variables x, y and z as depicted in Figure 19b. A negative clause is obtained by vertically mirroring the construction of a positive clause.

We now argue that the embedding of the graph $\mathcal{C}$ is planar and that the pairwise intersections of squares in the arrangement $\mathcal{D}_\mathcal{C}$ are empty. Observe that, every gadget is entirely embedded in the modified rectilinear representation. Recall that the rectilinear representation is planar and all gadget are placed in disjoint cells. Therefore, the pairwise intersection of squares in $\mathcal{D}_\mathcal{C}$ is empty. Moreover, each literal gadget is planar embedded in a single cell, each clause is embedded in a rectangle that covers five rows and six columns, and finally

each copy and inverter gadget together with its two literal gadget is embedded in either a single row and 3 columns or in 3 rows and a single column. Thus, since the modified rectilinear representation is planar and the pairwise intersections of squares in $\mathcal{D}_\mathcal{C}$ are empty, the graph $\mathcal{C}$ has a planar embedding. Finally, the maximal vertex degree of the literal gadget is three, the maximal degree a clause gadget is four. Connecting two literal gadgets by copy or inverter gadget increases the maximum vertex degree of $\mathcal{C}$ to five. Further, the obstacle number of the clause gadget is one and the obstacle number of the literal, copy and the inverter gadget is two.

It is left to show that the layout can be computed in polynomial time. As already argued the modified rectilinear representation Π of the monotone planar 3-SAT instance can be computed polynomial time. Moreover, the height and width of Π is linear in $|C|$. Thus, we inserted a number of gadgets linear in $|C|$. Further, the coordinates of each gadget are independent of the instance (U, C), thus overall the representation of the final arrangement $\mathcal{D}_\mathcal{C}$ is polynomial in $|U|$ and $|C|$. Placing a single gadget requires polynomial time, thus overall the clustered graph $\mathcal{C}$ and the arrangement $\mathcal{D}_\mathcal{C}$ of squares can be computed in polynomial time.

Correctness Assume that (U, C) is satisfiable. Depending on whether a variable u is true or false, we place all cycle vertices on a positive placement of a positive literal gadget and on the negative placement of negative literal gadget of the variable. Correspondingly, if u is false, we place the vertices on the negative and positive placements, respectively. By Property 3, the placement induces a $\mathcal{D}_\mathcal{C}$-framed drawing of all literal gadgets. Property 6 ensures that the copy and the inverter gadgets have a $\mathcal{D}_\mathcal{C}$-framed drawing. Since at least one variable of each clause is true, there is a $\mathcal{D}_\mathcal{C}$-framed drawing of each clause gadget by Property 8.

Now consider the clustered graph $\mathcal{C}$ has a $\mathcal{D}_\mathcal{C}$-framed drawing. Let X and Y be two positive literal gadgets or two negative literal gadgets connected with a copy gadget. By Property 4, a drawing of X is positive if and only if the drawing of Y is positive. Property 5 ensures that the drawing of a positive literal gadget X is positive if and only if the drawing of the negative literal gadget Y is negative, in case that both are joined with an inverter gadget. Further, Property 2 states that each cycle vertex lies either in a positive or negative region. Thus, the truth value of a variable u can be consistently determined by any drawing of a positive or negative literal gadget of u. By Property 8, the clause gadget has no $\mathcal{D}_\mathcal{C}$-framed drawing of the clause gadget such that all literal gadgets have a negative drawing. Thus, the truth assignment indeed satisfies C. □

4 Conclusion

We proved that every clustered planar graph with a pipe-disk intersection free disk arrangement $\mathcal{D}_\mathcal{C}$ and with a $\mathcal{D}_\mathcal{C}$-framed embedding ψ has a $\mathcal{D}_\mathcal{C}$-framed

straight-line drawing homeomorphic to ψ. In case of arrangements of unit disks and unit squares with pipe-disk intersections the problem becomes $\mathcal{NP}$-hard. This answers an open question of Angelini et al. [4]. We are not aware whether the problem is known to be in $\mathcal{NP}$. Due to the geometric nature of the problem, we ask whether techniques developed by Abrahamsen et al. [1] can be used to prove $\exists\mathbb{R}$-hardness. The cycles in the literal and copy gadget are crucial for our reduction. Thus, we ask whether the problem becomes tractable for restricted graph classes, e.g., trees, outerplanar graphs, or planar graphs that have maximum vertex degree 4.

References

[1] M. Abrahamsen, A. Adamaszek, and T. Miltzow. The Art Gallery Problem is $\exists\mathbb{R}$-complete. In *Proceedings of the 50th Annual ACM Symposium on Theory of Computing (STOC'18)*, pages 65–73. ACM Press, 2018. doi:10.1145/3188745.3188868.

[2] H. A. Akitaya, R. Fulek, and C. D. Tóth. Recognizing Weak Embeddings of Graphs. In Artur Czumaj, editor, *Proceedings of the 29th Annual ACM-SIAM Symposium on Discrete Algorithms (SODA'18)*, pages 274–292. Society for Industrial and Applied Mathematics, 2018. doi:10.1137/1.9781611975031.20.

[3] M. Alam, M. Kaufmann, S. G. Kobourov, and T. Mchedlidze. Fitting Planar Graphs on Planar Maps. *Journal of Graph Algorithms and Applications*, 19(1):413–440, 2015. doi:10.7155/jgaa.00367.

[4] P. Angelini, G. Da Lozzo, M. Di Bartolomeo, G. Di Battista, S.-H. Hong, M. Patrignani, and V. Roselli. Anchored Drawings of Planar Graphs. In C. Duncan and A. Symvonis, editors, *Proceedings of the 22nd International Symposium on Graph Drawing (GD'14)*, volume 8871 of *Lecture Notes in Computer Science*, pages 404–415. Springer Berlin/Heidelberg, 2014. doi:10.1007/978-3-662-45803-7_34.

[5] P. Angelini, F. Frati, and M. Kaufmann. Straight-Line Rectangular Drawings of Clustered Graphs. *Discrete & Computational Geometry*, 45(1):88–140, 2011. doi:10.1007/s00454-010-9302-z.

[6] B. Banyassady, M. Hoffmann, B. Klemz, M. Löffler, and T. Miltzow. Obedient Plane Drawings for Disk Intersection Graphs. In F. Ellen, A. Kolokolova, and J.-R. Sack, editors, *Proceedings of the 15th International Symposium on Algorithms and Data Structures (WADS'17)*, volume 10389 of *Lecture Notes in Computer Science*, pages 73–84, 2017. doi:10.1007/978-3-319-62127-2_7.

[7] T. Bläsius and I. Rutter. A New Perspective on Clustered Planarity as a Combinatorial Embedding Problem. *Theoretical Computer Science*, 609(2):306 – 315, 2016. doi:10.1016/j.tcs.2015.10.011.

[8] M. de Berg and A. Khosravi. Optimal Binary Space Partitions for Segments in the Plane. *International Journal of Computational Geometry & Applications*, 22(3):187–206, 2012. doi:10.1142/S0218195912500045.

[9] P. Eades, Q. Feng, X. Lin, and H. Nagamochi. Straight-Line Drawing Algorithms for Hierarchical Graphs and Clustered Graphs. *Algorithmica*, 44(1):1–32, 2006. doi:10.1007/s00453-004-1144-8.

[10] Q. Feng, R. F. Cohen, and P. Eades. Planarity for Clustered Graphs. In P. Spirakis, editor, *Proceedings of the Third Annual European Symposium on Algorithms (ESA'95)*, volume 979 of *Lecture Notes in Computer Science*, pages 213–226. Springer Berlin/Heidelberg, 1995. doi:10.1007/3-540-60313-1_145.

[11] M. Godau. On the Difficulty of Embedding Planar Graphs with Inaccuracies. In R. Tamassia and I. G. Tollis, editors, *Proceedings of the Second International Symposium on Graph Drawing (GD'94)*, volume 894 of *Lecture Notes in Computer Science*, pages 254–261. Springer Berlin/Heidelberg, 1995. doi:10.1007/3-540-58950-3_377.

[12] T. Mchedlidze, M. Radermacher, I. Rutter, and N. Zimbel. Drawing Clustered Graphs on Disk Arrangements. In *Proceedings of the 13th International Conference and Workshops on Algorithms and Computation (WALCOM '19)*, volume 11355 of *Lecture Notes in Computer Science*. Springer International Publishing, 2019. doi:10.1007/978-3-030-10564-8_13.

[13] A. Ribó Mor. *Realization and Counting Problems for Planar Structures*. PhD thesis, FU Berlin, 2006. URL: https://refubium.fu-berlin.de/handle/fub188/10243.